Statistical modeling to adjust for time trends in adaptive platform trials utilizing non-concurrent controls

Pavla Krotka¹, Martin Posch¹, Mohamed Gewily², Günter Höglinger^{3,4,5,6}, and Marta Bofill Roig^{*1}

¹Center for Medical Data Science, Medical University of Vienna, Vienna 1090, Austria

²Department of Pharmacy, Uppsala University, Uppsala, Sweden.

³Department of Neurology, LMU University Hospital, Ludwig-Maximilians-Universität (LMU) München, Munich, Germany.

⁴ German Center for Neurodegenerative Diseases (DZNE), Munich, Germany.
 ⁵ Munich Cluster for Systems Neurology (SyNergy), Munich, Germany.
 ⁶ Department of Neurology, Hannover Medical School, Hanover, Germany.

Abstract

Utilizing non-concurrent controls in the analysis of late-entering experimental arms in platform trials has recently received considerable attention, both on academic and regulatory levels. While incorporating this data can lead to increased power and lower required sample sizes, it might also introduce bias to the effect estimators if temporal drifts are present in the trial. Aiming to mitigate the potential calendar time bias, we propose various frequentist model-based approaches that leverage the non-concurrent control data, while adjusting for time trends. One of the currently available frequentist models incorporates time as a categorical fixed effect, separating the duration of the trial into periods, defined as time intervals bounded by any treatment arm entering or leaving the platform. In this work, we propose two extensions of this model. First, we consider an alternative definition of the time covariate by dividing the trial into fixed-length calendar time intervals. Second, we propose alternative methods to adjust for time trends. In particular, we investigate adjusting for autocorrelated random effects to account for dependency between closer time intervals and employing spline regression to model time with a smooth polynomial function. We evaluate the performance of the proposed approaches in a simulation study and illustrate their use by means of a case study.

1 Introduction

Platform trials accelerate drug development by offering increased flexibility and efficiency [1]. They evaluate the efficacy of multiple treatment arms under a single master protocol, with the added benefit of permitting treatment arms to enter the trial over time and to stop early based on interim data [2]. This design enables faster evaluation of drugs that are being developed, as they can be directly included to the shared platform [3]. Moreover, efficiency gains can be achieved by sharing the control group across the whole platform. The sharing of resources lowers the number of patients required in the control arm as well as the overall number of patients needed for the trial compared to stand-alone trials. This poses an advantage also from the ethical and patient perspective [4]. Given their complexity, designing platform trials requires extensive computer simulations and the use of software to assess their operating characteristics has become crucial for evaluating the robustness of the proposed design across different scenarios [5]. Moreover, valid statistical inference in platform trials remains of major concern to regulatory authorities, as several challenges arise due to the wide range of adaptive features, such as the late addition of experimental arms [6].

In particular, the use of the common control group in the statistical analysis of added arms has been a subject of lively discussions [7, 8, 9, 10]. In platform trials, for treatment arms that enter when the trial is

^{*}marta.bofillroig@meduniwien.ac.at

ongoing, the control group is divided into two separate groups: the concurrent controls (CC), which include patients that were randomized to the control arm at the same time as the given treatment arm was part of the platform trial and thus had a positive allocation probability of being randomized to the investigated treatment arm; and the non-concurrent controls (NCC), which denote patients randomized to the control group before the evaluated treatment arm entered the platform. Figure 1 exemplifies a platform trial with two experimental arms, where the second arm joined the trial at a later time point. NCC data for the second arm are marked with a diagonal striped pattern. Including NCC data in treatment-control comparisons can offer several benefits, such as a lower required sample size or increased statistical power compared to analysis based on concurrent controls only. However, since treatment arms are added sequentially, randomization occurs at different times. This lack of true randomization over time might lead to an inflation of the type I error rate and can introduce bias in the treatment effect estimators due to time trends. Time trends can be caused, for example, by changes in the standard of care, patient population, or seasonal effects [11].

Recently, several modeling approaches were proposed to overcome the challenge of leveraging the NCC data, while still controlling the type I error rate and without introducing bias to the effect estimators. Focusing on a platform trial with two experimental arms, Lee and Wason [8] and Bofill Roig et al. [9] considered frequentist modeling approaches, where time is included to the model either as a linear function, or a categorical covariate. For the latter, the trial is split into two periods, separated by the time point where the second experimental arm was added to the platform. It was shown that both models improve the statistical power as compared to the separate analysis and control the type I error rate, if the functional form of the time trend is correctly specified, the time trends are equal across all arms and additive on the model scale [9]. Moreover, the model with categorical adjustment asymptotically maintains the type I error rate even under misspecification of the functional form of the time trend, provided that block randomization is used. To deal with situations where time trends could differ between arms, Bofill Roig et al. [9] also investigated a model that includes interaction between treatment and time. However, while this model maintains the type I error rate also in cases with different time trends, the power gain from using NCC data is lost. A Bayesian alternative was suggested by Saville et al. [10] in their so-called Time Machine approach, which uses a Bayesian hierarchical model and adjusts for time in terms of intervals ("buckets") of equal length. The model smooths over the control response across the time buckets, such that closer buckets are modeled with more similar responses. They show that the Time Machine approximately controls the type I error rate and leads to superior performance in terms of statistical power as compared to the frequentist model with categorical adjustment for time in scenarios with linear time trend pattern. Marschner and Schou [12] proposed to analyze platform trials using meta-analysis techniques, which allow to conduct both treatment-control and treatment-treatment comparisons for non-concurrent arms. In this network meta-analysis approach, the platform trial is viewed as a network of direct (concurrent) comparisons, made within periods between trial adaptations; and indirect (non-concurrent) comparisons, made across multiple stages in the trial using a common reference arm. The estimates of the non-concurrent treatment-control comparisons are then obtained by linearly combining the direct contrast estimates.

In this work, we extend the frequentist modeling strategies from Bofill Roig et al. [9]. In particular, we propose an alternative definition of the time variable and consider adjusting for equally spaced calendar time intervals, similarly to the Bayesian Time Machine, also in the frequentist setting. Moreover, we investigate more advanced modeling approaches, such as mixed models or polynomial splines. The assumption of equal time trends, required for all methods proposed so far, may not always hold in practice, as temporal changes may affect treatment arms differently, e.g. in settings with different disease variants. Therefore, we investigate whether this assumption can be relaxed by considering a mixed model, which includes the interaction between treatment and time as a random effect. The performance of the proposed methods is evaluated in a simulation study, where we also assess the conditions under which the approaches lead to valid statistical inference. The use of the considered methods is demonstrated on a real-world dataset from a clinical trial for a rare disease progressive supranuclear palsy.

The remainder of this paper is structured as follows: Section 2 introduces the notation and considered trial design and describes the proposed methods for platform trials with equal time trends across all arms. In Section 3 we discuss a possible extension to trials where the temporal changes affect the arms differently. Section 4 presents an extensive simulation study, evaluating the operating characteristics of the considered methods under a wide range of settings. The use of the modeling strategies is exemplified in a case study using data on a rare neurodegenerative disease, presented in Section 5. We conclude the paper with a discussion

and conclusions in Section 6.

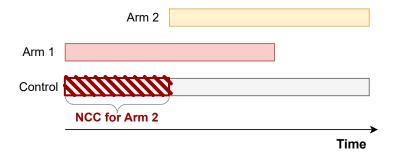


Figure 1: Non-concurrent control data for arm 2.

2 Methods

We consider a platform trial with a continuous endpoint that includes K experimental treatments ($K \ge 2$) and a shared control arm and assume that treatment arms enter the platform trial sequentially. We denote by k the treatment groups where k = 0 indicates the control and k = 1, ..., K the experimental treatment arms, indexed by entry order.

We consider two ways of splitting the time in the trial - into periods and calendar time intervals. The periods are defined as time intervals bounded by the time points where experimental treatment arms are added or dropped. Hence, alternations to the total number of arms currently involved in the trial always mark the start of a new period. The periods are indexed by $s=1,\ldots,S$, where S is the total number of periods. The time interval for period s is denoted by T_s^S ($s=1,\ldots,S$). An alternative to periods as defined above is to divide the trial duration into C equidistant units of calendar time (e.g. weeks or months), indexed by $c=1,\ldots,C$. We denote the calendar time intervals by T_c^C ($c=1,\ldots,C$) and their length by c_{length} . Figure 2 illustrates the division into periods and calendar time intervals in a platform trial with K experimental treatment arms and a shared control.

We focus on evaluating treatment arms that enter when the trial is already ongoing, and therefore, NCC data is available for these arms. We aim to compare the efficacy of each treatment against the control as soon as the treatment arm is completed, hence, no control data collected after the evaluated arm has finished is used in the analysis. Consider the one-sided null hypothesis $H_{0,M}: \theta_M \leq 0$ for arm M under study, where θ_M denotes the treatment effect size for treatment M against control. To test the null hypothesis $H_{0,M}$, we propose several model-based approaches.

To fit the proposed models, we use all data from the trial until treatment M leaves the platform. In other words, we use all data in the set $\mathcal{D}_M = \{(y_j, k_j, t_j), j=1,...,N \mid t_j \leq t_M^{exit}\}$, where j represents the patient index, y_j denotes the response, k_j and t_j are the arm and recruitment time corresponding to patient j, respectively, and t_M^{exit} marks the time point when the arm M left the trial. Note that also data from arms for which the recruitment is still ongoing at time t_M^{exit} is used to fit the models.

For technical definitions of the time variables, periods, and calendar time intervals, we refer to the supplementary material (see Sect. A).

In what follows, we introduce the proposed model-based approaches to test the null hypothesis $H_{0,M}$. These models incorporate the non-concurrent control data. The models adjust for time as a categorical fixed effect, a polynomial spline or a random factor, while stratifying time by either period or calendar time.

2.1 Fixed effect models

Firstly, we consider two linear regression models, which estimate the effect of treatments, which were active in the trial prior or up to the time unit t_M^{exit} and adjust for potential time trends by including time as a categorical covariate. The two approaches consider different definitions of the time variable, one using periods and the other one calendar time intervals.

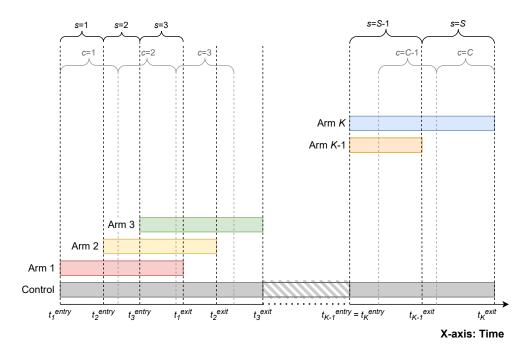


Figure 2: Example of a platform trial with K experimental treatment arms and a shared control group, illustrating the division of the trial duration into periods (denoted by s) and units of calendar time (denoted by c). The time points t_k^{entry} and t_k^{exit} (k = 1, ..., K) on the x-axis mark the entry and exit times of the experimental treatment arm k.

Period adjustment. As previously investigated by Lee and Wason [8] and Bofill Roig et al. [9] in simple platform trials with two experimental arms only, in the first model, we adjust for the time effect by including the factor "period" to the model, i.e., using a step-function:

$$y_j = \eta_{0,period} + \sum_{k \in \mathcal{K}_M} \theta_k \cdot I(k_j = k) + \sum_{s=2}^{S_M} \tau_s \cdot I(t_j \in T_s^S) + \varepsilon_j$$
 (1)

where $\eta_{0,period}$ is the response in the control arm in the first period; θ_k represents the effect of treatment k compared to control for $k \in \mathcal{K}_M$, where \mathcal{K}_M is the set of treatments that were active in the trial during periods prior or up to t_M^{exit} ; τ_s indicates the stepwise period effect between periods 1 and s ($s = 2, ..., S_M$), where $S_M = \{s \mid t_M^{exit} \in T_s^S\}$ denotes the period, in which arm M left the trial (i.e. the period in which t_M^{exit} is included).

Calendar time adjustment. In the second approach, analogously to the Bayesian Time Machine [10], we employ calendar time intervals to adjust for time trends. Specifically, we consider a regression model adjusting for the time effect by using calendar time intervals, and thus estimating the calendar time effect rather than period effect:

$$y_j = \eta_{0,calendar} + \sum_{k \in \mathcal{K}_M} \theta_k \cdot I(k_j = k) + \sum_{c=2}^{C_M} \tau_c \cdot I(t_j \in T_c^C) + \varepsilon_j$$
 (2)

Here $\eta_{0,calendar}$ represents the control response in the first calendar time unit; θ_k denotes the treatment effect of treatment k compared to control for $k \in \mathcal{K}_M$; τ_c is the stepwise effect between calendar time units 1 and c ($c = 2, ..., C_M$), where C_M indicates the calendar time unit, in which arm M left the trial. The length of the calendar time units c_{length} is given in terms of the number of enrolled patients and can be specified arbitrarily.

Note that both models (1) and (2) implicitly assume a time trend that is constant in all periods or calendar time intervals, respectively, and that the time effect is equal across all arms and additive on the model scale.

In both models, the residuals ε_j are assumed to follow a normal distribution $\varepsilon_j \sim \mathcal{N}(0, \sigma^2)$. However, the models take slightly different datasets into account - model (1) all trial data until the period S_M , model (2) all data until calendar unit C_M , which typically do not end at the same time. Moreover, the length of the time intervals in (2) poses an additional design parameter that allows to adjust for shorter time intervals than those given by the periods, which are also independent of the alternations to the trial design.

2.2 Spline regression

The models with a categorical fixed effect (1) and (2) assume that the time trend is constant within each period or calendar time interval. In order to also capture more complex patterns of the time trend, we consider estimating the patient response over time using spline regression. The model is given by:

$$y_j = \tilde{\eta}_0 + \sum_{k \in \mathcal{K}_M} \theta_k \cdot I(k_j = k) + f(t_j) + \varepsilon_j$$
(3)

where y_j , and θ_k are defined as in (1) and $\tilde{\eta}_0$ denotes the model intercept. The residuals are $\varepsilon_j \sim \mathcal{N}(0, \sigma^2)$. Note that the treatment effect enters the model as a linear predictor. The time trend is modeled via a continuous function $f(t_i)$ of the patient entry time t_i .

Specifically, we consider the B-spline function to model the time trend. This function is composed of multiple polynomial functions of a given degree q, which are joined together at points called knots, such that the entire spline is continuously differentiable up to the (q-1)th derivative [13]. For the positions of these knots, we evaluate two strategies, somewhat analogous to the period and calendar time adjustments. Firstly, we place the inner knots to the beginning of each period $s=2,\ldots,S$, such that one polynomial of degree q is always fitted to each period. Moreover, we consider placing the inner knots equidistantly, according to the length of the calendar time unit, and thus fitting a polynomial of degree q to each calendar time interval. Regarding the degree of the fitted polynomial, we explore linear, quadratic and cubic splines, i.e. $q \in (1, 2, 3)$. For details on the definition of the B-spline, see Sect. B.1 in the supplementary material.

Modeling the time using spline functions gives the model additional flexibility compared to the regression model that adjusts for time using a linear function considered in Lee and Wason [8] and Bofill Roig et al. [9], as now also more complex time trend patterns can be modeled more accurately.

2.3 Mixed effect models

In models (1) and (2), time is considered as a fixed factor. Alternatively, patients within different periods or calendar time units could be considered as different clusters, having a period- or calendar time-specific random intercepts. In what follows, we include the time variable to the models as a random factor. Under such models, the potential correlation between the random effects associated with different periods or calendar times can also be taken into account.

2.3.1 Mixed models with uncorrelated random effects.

First, we consider simple mixed effect models, where the effects of the given time intervals (period or calendar time units) are assumed to be uncorrelated with the effects of neighboring intervals. The mixed effect model with period adjustment has the following form:

$$y_j = \gamma_{0,period} + \sum_{k \in \mathcal{K}_M} \theta_k \cdot I(k_j = k) + \sum_{s=2}^{S_M} u_s \cdot I(t_j \in T_s^S) + \varepsilon_j$$
 (4)

whereas the model adjusting for calendar time units is given by:

$$y_j = \gamma_{0,calendar} + \sum_{k \in \mathcal{K}_M} \theta_k \cdot I(k_j = k) + \sum_{c=2}^{C_M} u_c \cdot I(t_j \in T_c^C) + \varepsilon_j$$
 (5)

where y_j and θ_k have the same interpretation as in the fixed effect models. The model intercepts $\gamma_{0,period}$ and $\gamma_{0,calendar}$ are, in this case, given in terms of the control response across the whole trial up until S_M

or C_M , respectively. u_s and u_c denote the random effect associated with the intercept for period s or calendar time unit c. These period- and calendar time-specific random effects are assumed to be normally distributed with mean 0 and constant variances σ_{period}^2 and $\sigma_{calendar}^2$, respectively: $u_s \sim \mathcal{N}(0, \sigma_{period}^2)$ and $u_c \sim \mathcal{N}(0, \sigma_{calendar}^2)$. Note that in this case, the correlation between any two period or calendar time effects is 0.

In both models, the distribution of the residuals ε_j , associated with the response of individual patient j is assumed to be the same for all treatments: $\varepsilon_j \sim \mathcal{N}(0, \sigma^2)$.

2.3.2 Mixed models with autocorrelated random effects.

To account for possible correlation of the random effects, we also consider random effects with first-order autoregressive structure (AR(1)), again with period or calendar time adjustments. The model equations are identical to (4) and (5).

There is a difference, however, with respect to the distribution of the random effects, which are now modeled as autocorrelated. Hence, the random effects for individual periods and calendar time units are assumed to be normally distributed with mean 0, constant variance σ_{period}^2 or $\sigma_{calendar}^2$, and an AR(1) correlation structure. For details, we refer to the supplementary material (see Sect. B.2). The model residuals ε_j are also assumed to be normally distributed (i.i.d.) with mean 0 and constant variance σ^2 .

3 Extension to relax the assumption of equal time trends

The modeling approaches outlined in the previous section, as well as all other modeling approaches available to date for utilizing non-concurrent controls, rely on the assumption of equal time trends in all arms in the platform trial on the model scale [14]. Violation of this assumption can lead to the loss of type I error rate control and biased treatment effect estimates. In this section, we propose an analysis method that could mitigate potential biases in trials where there are different time trends across arms.

In particular, we extend the mixed models from Section 2.3 and consider mixed models with treatment and time as categorical fixed effects (using the period definition of the time variable, as well as calendar time intervals) and the interaction between these variables as a random effect. The model adjusting for periods is defined as follows:

$$y_{j} = \eta_{0,period} + \sum_{k \in \mathcal{K}_{M}} \theta_{k} \cdot I(k_{j} = k) + \sum_{s=2}^{S_{M}} \tau_{s} \cdot I(t_{j} \in T_{s}^{S}) +$$

$$+ \sum_{k \in \mathcal{K}_{M} \setminus M} \sum_{s=2}^{S_{M}} u_{k,s} \cdot I(k_{j} = k) \cdot I(t_{j} \in T_{s}^{S}) + \varepsilon_{j}$$

$$(6)$$

Similarly, the model with calendar time adjustment is specified as:

$$y_{j} = \eta_{0,calendar} + \sum_{k \in \mathcal{K}_{M}} \theta_{k} \cdot I(k_{j} = k) + \sum_{c=2}^{C_{M}} \tau_{c} \cdot I(t_{j} \in T_{c}^{C}) +$$

$$+ \sum_{k \in \mathcal{K}_{M} \setminus M} \sum_{c=2}^{C_{M}} u_{k,c} \cdot I(k_{j} = k) \cdot I(t_{j} \in T_{c}^{C}) + \varepsilon_{j}$$

$$(7)$$

For the terms y_j , $\eta_{0,period}$, $\eta_{0,calendar}$, θ_k , τ_s and τ_c , the same interpretation as in the fixed effect models described in Section 2.1 holds. The interaction term between treatment arm and time interval is included as a random factor. Hence, the effects associated with treatment arm k ($k \neq M$) and period s (or treatment arm k ($k \neq M$) and calendar time unit c), denoted by $u_{k,s}$ and $u_{k,c}$, respectively, are drawn from a normal distribution with mean 0 and constant variances: $u_{k,s} \sim \mathcal{N}(0, \sigma^2_{arm,period})$ and $u_{k,c} \sim \mathcal{N}(0, \sigma^2_{arm,calendar})$ and are modeled as uncorrelated. Since it is assumed that the time trends in the evaluated treatment arm M and the control are equal, the arm M is excluded from the interaction term. As before, $\varepsilon_j \sim \mathcal{N}(0, \sigma^2)$ is assumed for the model residuals.

These models estimate the differences in the average response in each treatment arm relative to the control and each period/calendar time unit relative to the first one. Moreover, the interaction terms allow for a random variation in the response for each treatment arm in each period/calendar time unit. As the random effects are centered around 0, this approach is shrinking this random variation towards 0. While under different time trends, this approach may not completely remove the bias (due to the shrinkage), it is expected to reduce the bias compared to a model without the interaction term.

4 Simulation study

We evaluate the properties of the methods proposed in Sections 2 and 3 in a simulation study and discuss the influence of certain design parameters on the type I error rate and statistical power.

4.1 Design

We consider a platform trial with K experimental treatment arms that enter the trial sequentially and a control group that is common to all treatment arms. In the simulations, we assume that the recruitment is uniform with exactly one patient being enrolled at each time point. The timing of adding of the treatment arms can then be expressed in terms of the cumulative sample size, given by $\mathbf{d} = (d_1, \dots, d_K)$, where d_k indicates how many patients had already been enrolled to the trial by the time treatment k entered the platform. Note that in this special case of uniform patient recruitment, we have $t_k^{entry} = d_k$. We always set the d_1 to 0 to ensure that the platform trial starts with at least one experimental treatment. In this work, we consider platform trials with equidistant entry times of the experimental treatment arms, where the arm k enters the trial after $d_k = d \cdot (k-1)$ patients have been recruited to the platform. Note that the parameter d determines the amount of overlapping sample size between the treatment arms. If d = 0, all arms join and leave the trial simultaneously, resulting in a standard multi-arm trial and a total overlap between the arms. If d = 2n, a new treatment arm enters the trial once the previous one finishes, so that there is only one active experimental arm at a time, and hence no overlap between them.

4.1.1 Data generation

To generate the trial data we assume an allocation ratio of $1:1:\dots:1$ in each period. Patients are assigned to arms following block randomization with block sizes of $2 \cdot (\text{number of active arms} + 1)$ at each time t. Patients are indexed by entry order, assuming that at each time unit exactly one patient is recruited (i.e., $t_j = j$) and the time of recruitment and of the observation of the response are equal. The continuous outcome y_j for patient j is then drawn from a normal distribution according to $y_j \sim \mathcal{N}(\mu, \sigma^2)$ with

$$\mu = \eta_0 + \sum_{k=1}^{K} \theta_k \cdot I(k_j = k) + f(j) \text{ and } \sigma^2 = 1$$

where η_0 and θ_k are the response in the control arm and the effect of treatment k. Moreover, time trends of various strengths and shapes may be present in the trial. The time trends are denoted by the function f(j) and their magnitude is arm k is parameterized by λ_k . The following time trend patterns are considered:

Inverted-U time trend: $f(j) = \lambda_k \cdot \frac{j-1}{N-1}$ for $j \leq N_p$ and $f(j) = -\lambda_k \cdot \frac{j-N_p}{N-1} + \lambda_k \cdot \frac{N_p-1}{N-1}$ for $j > N_p$, where N indicates the total sample size in the trial and N_p is the point at which the trend turns from positive to negative in terms of the sample size. For $\lambda_k > 0$ the mean response in arm k linearly increases (with slope λ_k) until the total sample size has reached N_p , and linearly decreases afterwards. For $\lambda_k < 0$, it decreases until N_p and increases afterwards.

Linear time trend: $f(j) = \lambda_k \cdot \frac{j-1}{N-1}$, where N indicates the total sample size in the trial. The mean response in arm k linearly increases with the slope λ_k over time.

Seasonal time trend: $f(j) = \lambda_k \cdot \sin(\psi \cdot 2\pi \cdot \frac{j-1}{N-1})$, where N indicates the total sample size in the trial. The seasonal trend may consist of multiple cycles, where the response increases at first and decreases afterwards, while the respective peaks of the cycles correspond to λ_k or $-\lambda_k$. The number of cycles over the whole platform trial is determined by ψ .

Stepwise time trend: $f(j) = \lambda_k \cdot (i_j - 1)$, where i_j indicates how many treatment arms have already entered the trial at the time patient j was enrolled. Hence, there is a jump in the mean response in arm k of size λ_k every time a new arm is added to the trial. If multiple arms are added simultaneously, the jump in the response is multiplied by how many arms have entered. Note that the stepwise time trend is in general stronger than the other patterns and hence not directly comparable to them. This is in particular pronounced in trials with many treatment arms, as the trend increases by λ_k every time a new arm enters the platform. The rationale behind considering this pattern in the simulations is to examine the behavior of the models in more extreme situations.

The considered time trend patterns are illustrated in Figure 3.

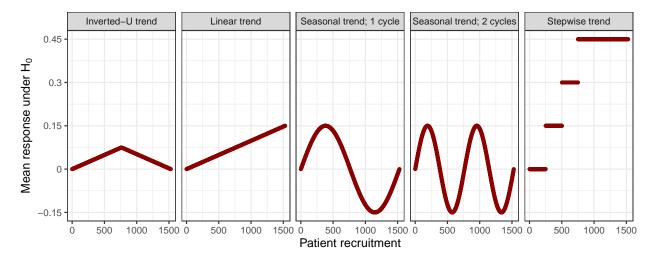


Figure 3: Mean responses under the null hypothesis under time trends of different patterns and strength of $\lambda_k = 0.15 \ \forall k$ in a platform trial with 4 experimental treatment arms entering the trial sequentially.

4.1.2 Considered trial settings

We distinguish three settings in which we vary the design according to the objectives of the simulation study: **Setting 1:** With the objective of assessing the impact of the overlap between arms, we focus on a larger platform trial with K = 10 experimental arms and equal time trend in all arms $(\lambda_k = \lambda_0 \ \forall k)$. We compare arm M = 5 to the control, while varying the strength of the time trend (λ_k) .

Setting 1A: Focusing on trials with a linear time trend, here, we additionally vary the amount of overlap between the treatment arms by varying the entry times. In this setting, we evaluate the impact of the overlapping sample size on the performance of the fixed effect regression model with period adjustment (1).

Setting 1B: Here, we additionally vary the pattern of the time trend, considering all time trend shapes listed above. In this setting, we assess the properties of the spline regression (3) under different time trend patterns with varying strengths.

Setting 2: In order to understand the behavior of the fixed effect model using the alternative definition of time, as well as the mixed effect models, it is sufficient to investigate a simpler platform trial with K=4 experimental arms and equal time trend in all arms $(\lambda_k = \lambda_0 \ \forall k)$. We compare arm M=3 to the control, while varying the pattern (considering all patterns listed above) and strength of the time trend (λ_k) .

Setting 2A: Here, we additionally vary the size of the calendar time unit, in order to examine the influence of this parameter on the operating characteristics of the fixed effect model adjusting for calendar time (2). We compare the performance of this model to the fixed effect model with period adjustment (1).

Setting	K	d	λ	Trend pattern	Calendar time unit size	Objective	
1A	10	$d_k = d \cdot (k-1) \ \forall k \ge 1$ $-d \in [0, 500]$ - with increments of 25	$\lambda_k = \lambda_0 \in [-0.5, 0.5] \; \forall k$ - with increments of 0.125	Linear	-	Evaluate the fixed effect regression model with period adjustment (1)	
1B	10	$d_k = d \cdot (k-1) \ \forall k \ge 1$ $-d = 250$	$\lambda_k = \lambda_0 \in [-0.5, 0.5] \ \forall k$ - with increments of 0.125	Linear, stepwise, inverted-U seasonal	100	Evaluate the spline regression (3)	
2A	4	$d_k = d \cdot (k-1) \ \forall k \ge 1$ $-d = 250$	$\lambda_k = \lambda_0 \in [-0.5, 0.5] \; \forall k$ - with increments of 0.125	Linear, stepwise, inverted-U seasonal	[25, 750] with increments of 25	Evaluate the definition of time as calendar time intervals in the fixed effect model (2)	
2B	4	$d_k = d \cdot (k-1) \ \forall k \ge 1$ $-d = 250$	$\lambda_k = \lambda_0 \in [-0.5, 0.5] \; \forall k$ - with increments of 0.125	Linear, stepwise, inverted-U seasonal	100	Evaluate the mixed models without interaction (4), (5)	
3	4	$d_k = d \cdot (k-1) \ \forall k \ge 1$ $-d = 250$	1) $\lambda_1 \in [-0.5, 0.5];$ $\lambda_0 = \lambda_2 = \lambda_3 = \lambda_4 = 0$ 2) $\lambda_1 = \lambda_2 \in [-0.5, 0.5];$ $\lambda_0 = \lambda_3 = \lambda_4 = 0$ 3) $\lambda_1 = \lambda_2 = \lambda_4 \in [-0.5, 0.5];$ $\lambda_0 = \lambda_3 = 0$ 4) $\lambda_1 \in [-0.5, 0.5];$ $\lambda_2 = 2\lambda_1;$ $\lambda_4 = 3\lambda_1;$ $\lambda_0 = \lambda_3 = 0$ 5) $\lambda_k = \lambda_0 \in [-0.5, 0.5] \ \forall k$ - intervals with increments of 0.125	Linear	100	Evaluate the mixed models with interaction (6), (7)	

Table 1: Simulation settings and parameters considered in the simulation study.

Setting 2B: Using calendar time unit size of 100 patients, in this setting we evaluate the performance of the mixed effect models without interaction ((4) and (5)). Considering different time trend patterns with varying strength, we compare these models to the fixed effect model adjusting for periods (1).

Setting 3: Keeping the platform trial with K=4 experimental arms from the previous setting, we focus on examining trials with different time trends across arms. Again, we compare arm M=3 to the control, while varying the pattern (considering all patterns listed above) and strength of the time trend (λ_k) . In particular, the treatment arm 3 and the control group have no time trend $(\lambda_0 = \lambda_3 = 0)$, while the rest of the arms have time trends of different strengths. We vary the strength of the time trend in arms 1 $(\lambda_0 = \lambda_2 = \lambda_3 = \lambda_4 \neq \lambda_1)$, 1 and 2 $(\lambda_0 = \lambda_3 = \lambda_4 \neq \lambda_1 = \lambda_2)$, or 1, 2 and 4 $(\lambda_0 = \lambda_3 \neq \lambda_1 = \lambda_2 = \lambda_4)$ and $(\lambda_0 = \lambda_3 \neq \lambda_1)$. In this setting, we evaluate the performance of the mixed effect models with interaction ((6) and (7)) and compare it to the fixed effect model adjusting for periods (1).

In all cases, we assume an underlying mean response of zero for the control arm ($\eta_0 = 0$) and a treatment effect of $\theta_k = 0.25$ for treatment arms under the alternative hypothesis, as well as sample sizes of n = 250 for all experimental treatment arms. This treatment effect was chosen such that the analysis using CC data only achieves approximately 80% power with the given sample size at a one-sided significance level $\alpha = 0.025$.

For comparative purposes, we also analyze the data with two simple standard approaches, where the data from the investigated treatment arm M is compared either to pooled NCC and CC data (pooled analysis) or only CC data (separate analysis) with one-sided t-tests [15]. Moreover, we include the fixed effects model with period adjustment (1) as a reference model for all comparisons.

Table 1 summarizes the considered simulation settings and parameters. We simulated 10,000 replicates of each scenario to estimate the type I error rate and statistical power.

4.2 Results

For better legibility and easier comparison, we restricted the range of the y-axis in all plots showing the statistical power to [0.7, 1]. If the power is not visible for some values on the x-axis, the estimated power was below 0.7. In all plots showing the estimated type I error rate, we include a dashed reference line for the nominal significance level of 0.025 and a grey area around this value representing the 95% prediction interval of the simulated type I error rate with 10,000 simulation runs, provided that the true type I error rate is 0.025.

4.2.1 Setting 1: Assessing the properties of the fixed effect model with period adjustment and of the spline regression

Considering a platform trial with 10 experimental treatment arms and a shared control arm, we assess the operating characteristics of the fixed effect model adjusting for periods and the spline regression. In particular, we evaluate the effect of the overlapping sample size and the strength and pattern of the time trend on the type I error rate and statistical power.

Setting 1A. Figure 4 shows the impact of the strength of the time trend on the operating characteristics when evaluating treatment arm 5. Analogous plots for all treatment arms can be found in Figure S1 in the supplementary material. The regression model, as well as the separate analysis asymptotically control the type I error rate, regardless of the strength of the time trend. The pooled analysis leads to inflation of the type I error in the presence of positive time trends and deflation in case of negative time trends. Although only results for linear time trends are shown, the regression model maintains the type I error rate under arbitrary time trend pattern. Additionally, the model leads to gains in power as compared to the separate analysis. This result is in line with previous works [8, 9].

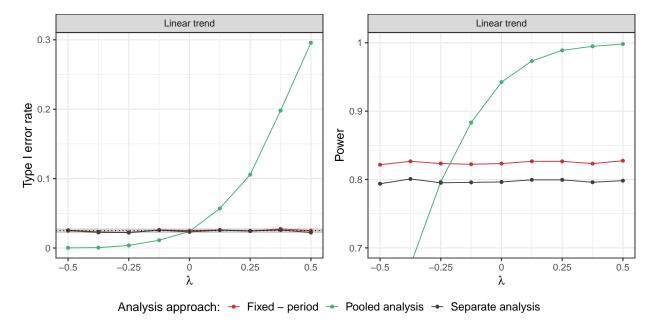


Figure 4: Setting 1A: Type I error rate and power of the fixed effect regression model with period adjustment compared to the pooled and separate analyses with respect to the strength of the time trend λ . Here, d = 400, n = 250 in each experimental arm, and a linear shape of the time trend are used. Treatment arm 5 is being evaluated.

We vary the overlap between arms by varying the parameter d from 0 to 2n = 500. The effect of the amount of overlapping sample size when evaluating treatment arm 5 is shown in Figure 5. Figure S2 in the supplementary material shows analogous plots for all treatment arms. The overlaps do not affect the type I error rate control of the regression model and separate approach, which is guaranteed (asymptotically) in all

the cases. The inflation of the pooled analysis gets stronger with increasing d. This is because larger values of d result in longer platform trials and larger size of the NCC data. The power of the regression model, however, depends on the overlap between treatment arms. In the extreme cases with d=0 and d=2n, the regression model leads to identical power as the separate analysis. If d=0, there is no NCC data, as all the arms join the trial at the beginning. Thus, the control group used for the treatment-control comparison is the same for both, the separate analysis and the regression model. In case of no overlap between the arms (d=2n=500), there is insufficient amount of data to estimate the period effect. Hence, simultaneous presence of the experimental arms in the trial is crucial for a reliable estimation of the period effect and resulting power gains when using the regression model. For the considered simulations, the maximal power is reached for d=175, which in this case leads to the optimal trade-off between the amount of overlapping sample size between treatment arms and the size of the non-concurrent data.

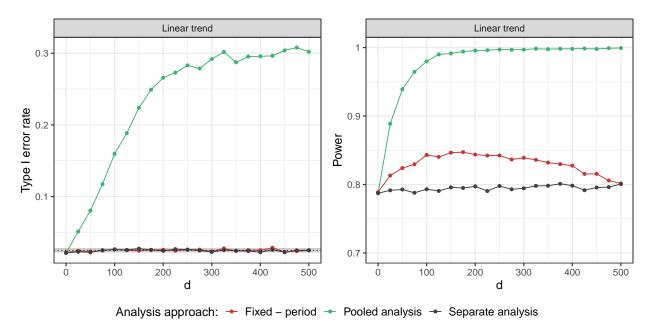


Figure 5: Setting 1A: Type I error rate and power of the fixed effect regression model with period adjustment compared to the pooled and separate analyses with respect to the timing of adding the treatment arms. Here, n = 250 in each experimental arm and a linear time trend with strength $\lambda = 0.5$ are considered. Treatment arm 5 is being evaluated.

Figure S3 in the supplementary material illustrates how the type I error rate and power for individual treatment-control comparisons depends on the order of entry in the platform trial. We observe that the power of the regression model increases for arms that were added to the trial later. This is due to larger sample size of the NCC data. On the other hand, this also leads to a higher inflation of the type I error with the pooled analysis.

Setting 1B. To evaluate the performance of the spline regression, we focused on a platform trial where arm k is added after every $d_k = 250 \cdot (k-1)$ patients have been enrolled in the trial. Here, we also varied the degree of the B-splines in the simulations, considering linear, quadratic, and cubic splines. However, since the differences in the resulting operating characteristics were only marginal, here we only present results for the cubic spline regression. The knots are placed either at the beginning of each period or each calendar time interval. Results for linear and quadratic splines can be found in supplementary Figure S4.

The type I error rate and power of the evaluated models under the considered scenarios when comparing treatment arm 5 to the control are presented in Figure 6. Analogous plots for other experimental arms are given in Figure S5 in the supplement. If the time trend pattern is given by a continuous function, the spline regression maintains the type I error rate. However, in case of the stepwise time trend, we observe an inflation in the type I error rate, particularly pronounced when placing the knots according to the periods. This is because the spline regression estimates the time effect by a smooth function, composed of multiple

polynomial functions joined together in the knots. This is not an optimal approach if there are sudden jumps in the time trend. Note that the separate approach has a type I error rate strictly below 2.5% for strong time trends under the seasonal trend pattern and in particular under the stepwise trend pattern, as this one has stronger values than the other shapes. The reason is that block randomization was used to assign the patients to the active arms. In case of very strong time trends, ignoring the blocks in the analysis results in a conservative test, as the variances of the treatment effects are overestimated. This leads to deflation in the type I error rate, which gets stronger the more extreme the time trend is [16].

The power of the spline regression in cases with continuous time trend function is slightly improved as compared to the fixed effects model, however, the differences are only marginal in the considered scenarios.

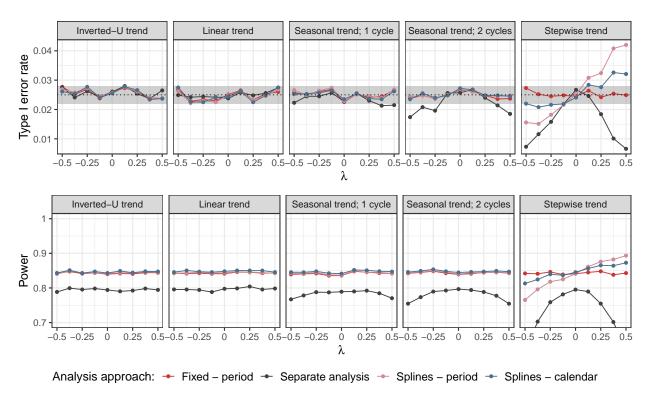


Figure 6: Setting 1B: Type I error rate and power for the cubic spline regression model with knots according to periods or calendar time units compared to the regression model with period adjustment with respect to the strength of the time trend λ using different time trend patterns. Here, n=250 in each experimental arm and $N_p=1660$ in case of inverted-U trend (corresponding to the middle of the trial) are used. In case of calendar time adjustment, unit size of 100 patients is considered. Treatment arm 5 is being evaluated.

4.2.2 Setting 2: Comparing the calendar time adjustment to the period adjustment in the fixed effect models and evaluating the mixed models without interaction

To examine the regression model with calendar time adjustment and the mixed models without interaction, we consider a platform trial with 4 experimental treatment arms, where arm k enters after $d_k = 250 \cdot (k-1)$ patients have been recruited to the trial, leading to a total sample size of 1528 patients. We focus on evaluating treatment arm 3 and assess how the model performance depends on the pattern and strength of the time trend, as well as on the chosen calendar time length.

Setting 2A. In Figures 7 and 8 the type I error rate and power of the model with the calendar time adjustment is compared to the period adjustment and the separate analysis under varying unit size and λ , respectively. Corresponding results for other experimental arms are presented in Figures S6 and S7 in the supplementary material. For Figure 7, unit sizes in the range from 25 to 750 (see Table 1) were considered. The type I error rate control for different time unit lengths is dependent on the time trend pattern. In case of linear and inverted-U trend, the type I error rate is maintained for moderately sized calendar time units, and slightly inflated for units larger than 600 patients. Under the seasonal time trend, we observe deflation of the type I error for unit sizes ≥ 200 . In case of the stepwise trend, the type I error rate control is only given for very small unit sizes (< 50 patients). The loss of type I error rate control for larger calendar unit sizes is due to the fact that larger unit sizes lead to greater pooling of the concurrent and non-concurrent data. In trials with sudden changes in the time trend (such as the considered stepwise trend pattern), the type I error inflation for naive pooling is more pronounced, therefore the control is only given for smaller sizes. The type I error rate would be controlled in settings with stepwise trend if treatment arms were only allowed to enter the trial at the beginning of a calendar time unit. This, however, was not the case in our simulations. Depending on the unit size, the model with calendar time adjustment can lead to power improvements as compared to the period adjustment, especially in the setting with inverted-U or linear time trend. Nevertheless, as the type I error rate is not maintained in all cases, the choice of the interval length and the resulting trade-off between type I and type II errors needs to be carefully assessed.

Setting 2B. Similarly, for the evaluation of the mixed models without interaction, we focus on evaluating treatment arm 3, consider varying time trend patterns and strengths, and present the resulting type I error rate and power in Figure 9. Figure S8 in the supplementary material shows corresponding results for other treatment arms.

We observe that the mixed models only maintain the type I error rate if no time trends are present in the trial (i.e., $\lambda=0$). Under this assumption, they also lead to power improvement compared to the fixed effect regression model. However, in case of time trends the type I error rate control is lost. The inflation (or deflation) of the type I error is most pronounced in the mixed model that adjusts for calendar time intervals as uncorrelated random effects. This is because the variance of the random effects is underestimated since fewer observations are available in each calendar time interval, and the observations within one interval are more similar to each other than it is the case for the periods. Moreover, especially in settings with seasonal and stepwise trends, the maximum inflation seems to be achieved for moderately strong time trends. The reason for this is that the mixed models shrink the effect of the time trend, since it is modeled as a random effect. If, however, the trend is large enough, there is less shrinkage and the time effect is preserved and better adjusted for.

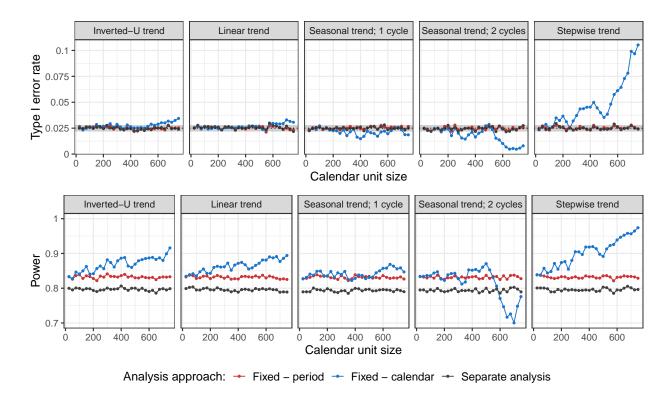


Figure 7: Setting 2A: Type I error rate and power of the regression model with calendar time adjustment compared to the regression model with period adjustment and separate analysis with respect to the size of the calendar time unit under different time trend patterns. Here, n=250 in each experimental arm, $\lambda=0.125$, and $N_p=750$ in case of inverted-U trend (corresponding approximately to the middle of the trial) are considered. Treatment arm 3 is being evaluated.

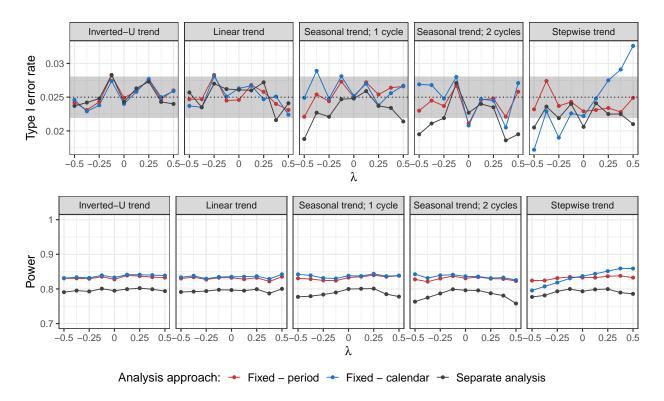


Figure 8: Setting 2A: Type I error rate and power of the regression model with calendar time adjustment compared to the regression model with period adjustment and separate analysis with respect to the strength of the time trend λ under different time trend patterns. Here, n=250 in each experimental arm, $N_p=750$ in case of inverted-U trend (corresponding approximately to the middle of the trial), and calendar time unit size of 100 are used. Treatment arm 3 is being evaluated.

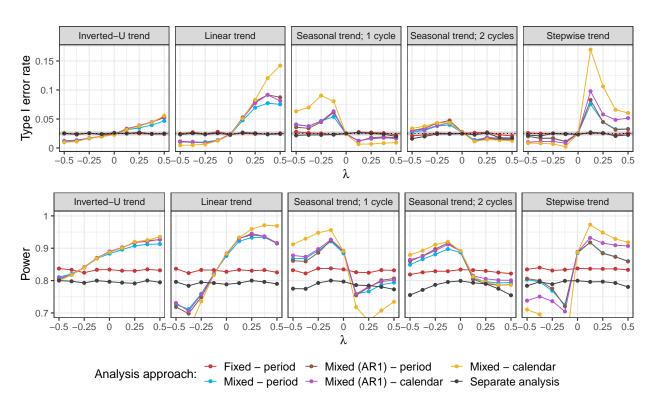


Figure 9: Setting 2B: Type I error rate and power of the mixed model with period and calendar time adjustments as uncorrelated and autocorrelated random effects, compared to the fixed effect regression model with period adjustment with respect to the pattern and strength of the time trend. Sample sizes of n=250 in each experimental arm and $N_p=750$ in case of inverted-U trend (corresponding approximately to the middle of the trial) are assumed. In case of calendar time adjustment, unit size of 100 patients is considered. Treatment arm 3 is being evaluated.

4.2.3 Setting 3: Evaluating the performance of the mixed models with interaction under different time trends

To evaluate whether the mixed models with interaction reduce the type I error rate inflation under different time trends, we consider a scenario with K=4 experimental arms where treatment arm 3 is being evaluated, as in Setting 2. In this case, only the linear pattern of the time trend is considered. However, we simulate different cases with regard to the strength of the time trend. In particular, we vary the strength of the time trend in arm 1 (λ_1), arms 1 and 2 ($\lambda_1 = \lambda_2$) or arms 1, 2 and 4. In the last case, we additionally distinguish between two variants - equal time trend strengths in arms 1, 2, and 4 ($\lambda_1 = \lambda_2 = \lambda_4$) and different strengths across these arms ($\lambda_2 = 2\lambda_1$, $\lambda_4 = 3\lambda_1$). The remaining arms have no time trend. For comparison, we also consider a case with equal time trends in all arms ($\lambda_1 = \lambda_k, \forall k$).

Figure 10 shows the obtained type I error rate and power with respect to λ_1 for the two variants of the mixed model with interaction (adjusting for period or calendar time units), compared to the fixed effect model with period adjustment and the separate analysis. Different cases regarding the strength of the time trend are presented in the columns. The results show that the mixed models lead to less inflation than the fixed effect model in the case of different time trends. The improvement in the type I error rate inflation when using the mixed models compared to the fixed effect model is particularly pronounced in the case with more variation in the time trend strength across arms (see Figure 10, 4th column). However, as expected, the mixed effect models do not maintain the type I error rate at the nominal level for arbitrary strengths of the time trend. In the case of equal time trends, they control the type I error rate and lead to comparable power as the fixed effect model with period adjustment.

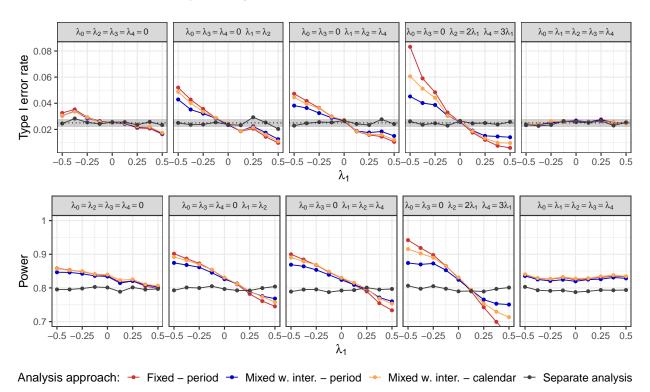


Figure 10: **Setting 3:** Type I error rate and power of the mixed model with interaction and period or calendar time adjustments, compared to the fixed effect regression model with period adjustment with respect to the time trend case and its strength. Sample sizes of n = 250 in each experimental arm are assumed. In case of calendar time adjustment, unit size of 100 patients is considered. Treatment arm 3 is being evaluated.

4.3 Implementation

The simulation study was performed using the NCC R package [17], which contains functions implementing all considered analysis approaches, as well as functions for data simulation and performing simulation studies [18].

5 Case Study

We exemplify the use of the proposed methods on data from the ABBV-8E12 trial [19] for Progressive Supranuclear Palsy (PSP), a rare neurodegenerative disorder affecting balance, body movements, vision, and speech, eventually resulting in death. The ABBV-8E12 study evaluated the safety and efficacy of different doses (2000mg - here denoted as arm 1; and 4000mg - denoted as arm 2) of the experimental treatment Tilavonemab in a randomized parallel group trial, using placebo as a common control group. The trial recruited patients over a period of approximately 2 years, from January 2017 to March 2019. When revisiting this data, we consider the Progressive Supranuclear Palsy Rating Scale (PSPRS) as an endpoint, a sum score summing up the values for 28 different items, which measure the progression of the disease across different domains (lower values of this score indicate better outcomes) [20]. To demonstrate the potential impact of time trends under the null hypothesis, for illustrative purposes we compare the baseline measurements of the sum score between treatment and control groups (instead of the change from baseline as in the original trial). For the baseline measurements, we know that due to randomization there is no treatment effect compared to placebo for both arms, such that all observed treatment effects are either due to bias or sampling error. We furthermore demonstrate the use of the proposed models on this data.

To emulate a two-period platform trial, we modified the original multi-arm trial data and assumed that the second experimental arm (4000mg of Tilavonemab) enters the ongoing trial at a later time point. Therefore, we set the cut-off for the periods (i.e., the time point where treatment arm 2 enters the platform) to 1.6.2018 and exclude observations from patients allocated to arm 2 prior to this cut-off date from the analysis. The resulting dataset consists of 315 patients, with sample sizes of 123, 126, and 66 for the placebo arm, and treatment arms 1 and 2, respectively. For approaches that adjust for calendar time, we use a unit length of 90 days, which divides the trial into 9 calendar time units, each of them corresponding to approximately 3 months. Note that as the patient recruitment was not uniform, the numbers of patients in each unit are different, ranging from 4 in the first unit to 96 in the 8th. Figure 11 visualizes the considered data, showing the division into periods (red dashed line) and calendar time units (grey dashed lines).

First, we investigate the presence of a possible time trend in the modified trial data by fitting a linear model to the primary outcome, using treatment as categorical, and days since the recruitment of the first patient as continuous covariates. Fitted values from this model are included as solid lines in Figure 11. The model showed a significant negative time trend (p=0.032), which is also visible in the figure. Hence, at the beginning, the trial recruited patients with more severe stage of the disease, while participants recruited later had on average a milder stage of PSP.

Subsequently, we analyze the dataset using the proposed modeling approaches, as well as the separate and pooled analyses, and compare the estimated treatment effects, their standard errors, and p-values. In the case of the mixed models, we only consider the calendar time adjustment, as the analyzed trial only consists of two periods, which would lead to a very unstable estimation of the random effect in case of the period adjustment. We focus on evaluating the efficacy of the 2nd experimental arm against control, since this arm has non-concurrent control data available. Table 2 summarizes the obtained results. Since the considered responses were measured at the baseline date in a randomized trial, we can assume that the null hypothesis holds, thus the underlying treatment effect is 0 for both arms. We evaluate this null hypothesis $(H_{0.2}:\theta_2=0)$ against the two-sided alternative $(H_{1,2}:\theta_2\neq 0)$. None of the analysis approaches reject the null hypothesis. The most accurate estimate of the treatment effect (-0.0123) is provided by the fixed effect model adjusting for periods, followed by the fixed effect model with calendar time adjustment (-0.0682). These models also result in the highest p-values against the null hypothesis (p=0.995 and p=0.971, respectively). The second closest estimate is provided by the spline regression, resulting in estimated effects of 0.1795 and 0.6239 for the period and calendar time adjustment, respectively. In both model classes (fixed effect models and spline regressions), the period adjustment leads to a better effect estimate than the calendar time adjustment. The standard errors of the estimates are comparable for all considered models, ranging from 1.8223 (mixed model

Analysis approach	${f Adjust ment}$	Effect estimate	Std. error	p-value
Fixed effect model	Periods	-0.0123	1.8961	0.995
r ixed effect filodei	Calendar time units	-0.0682	1.9002	0.971
Mixed model	Calendar time units	-0.9028	1.8326	0.623
Mixed model (AR1)	Calendar time units	-0.9730	1.8223	0.594
Spline regression	Periods	0.1795	1.8851	0.924
Spinie regression	Calendar time units	0.6239	1.8794	0.740
Pooled analysis	-	-1.7030	1.7660	0.336
Separate analysis	-	-0.4104	2.0323	0.840

Table 2: Treatment effect estimates, standard errors and two-sided p-values obtained when comparing the second treatment arm against the control using the proposed approaches.

with autocorrelated random effects and calendar time adjustment) to 1.9002 (fixed effect model with calendar time adjustment). We can also observe that all modeling approaches yield estimates that are closer to the true effect than the pooled analysis, which introduces a considerable bias to the effect estimation (-1.7030) and also provides the lowest p-value (p=0.336).

In the ABBV-8E12 trial, the primary endpoint was the change from baseline in the PSPRS score after 52 weeks. We also investigated potential time trends for this endpoint, but observed no substantial drift in this outcome during the trial (data not shown). Hence, this data suggests that time trends would not pose a problem in this particular trial, and the fact that patients with a milder stage of PSP were recruited later in the trial is accounted for by adjusting for the baseline response. For an assessment of the efficiency of other choices for the primary endpoint see Yousefi et al. [21].

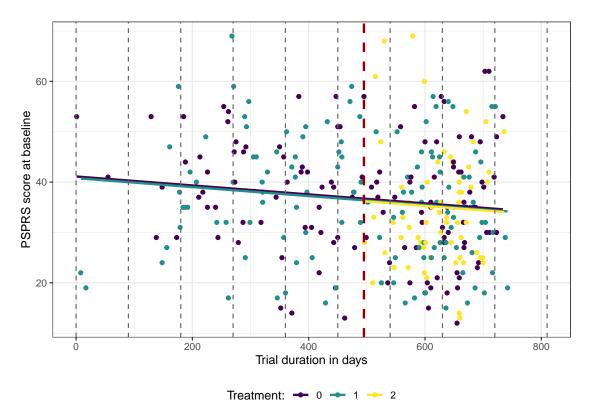


Figure 11: Data from the ABBV-8E12 trial: responses measured at baseline. The data was modified to resemble a platform trial consisting of two periods (indicated by the red dashed line) and nine calendar time units (denoted by the grey dashed lines).

6 Discussion

The use of non-concurrent controls in the analysis of platform trials has been the subject of discussions and intense methodological research during recent years. In this work, we extended the currently available frequentist methods and proposed novel, model-based approaches to utilize non-concurrent controls for individual treatment-control comparisons. We introduced an alternative definition of the time covariate in the frequentist models, where the duration of the trial is divided into calendar time intervals of equal length. This is analogous to the time buckets considered in the Bayesian "Time Machine" approach [10]. Moreover, we considered more flexible means of modeling the time trend. In particular, we proposed adding the time covariate as a random effect in a linear mixed model. In these models, we additionally allowed for autocorrelation between the random effects in order to account for dependency between closer time intervals. Furthermore, we employed B-splines to model time with a polynomial function in a spline regression. Here we considered two options of placing the inner knots - either according to the periods in the trial or according to the calendar time intervals. To relax the assumption of equal time trends crucial for all previously considered methods, we proposed an extension of the modeling approaches, where we included treatment and time as fixed effects and the interaction between them as a random effect.

We evaluated the performance of the proposed methods in terms of the type I error rate and statistical power in a simulation study, considering a wide range of scenarios. We specified under which conditions the fixed effect model adjusting for periods leads to power gains as compared to the separate analysis. Moreover, we showed that the calendar time adjustment in fixed effect models can, in some scenarios, lead to power gains as compared to the period adjustment while still controlling the type I error rate. In the considered scenarios, the mixed models without interaction were not suitable for evaluating the efficacy of late-entering treatment arms in the presence of time trends, as they do not preserve the type I error rate. Lee and Wason [8] and Bofill Roig et al. [9] investigated a linear regression model that includes time as a continuous, rather than categorical variable. It was shown that this model only controls the type I error rate if the underlying time trend has a linear pattern. The spline regression can be viewed as a generalization of this model, fitting one polynomial function for each period or calendar time interval, rather than one linear function for the whole trial, to adjust for time. We demonstrated via simulations that modeling time via a spline function controls the type I error rate for all considered scenarios with continuous time trends. Furthermore, it was shown that the models with fixed factor period that also include a term for interaction between treatment and time as a random effect, can improve the robustness and decrease the inflation of the type I error rate compared to the model without this interaction, if the time trends are not equal across arms. The proposed analysis approaches focus only on trials with continuous endpoints. The extension of the presented methods to other types of endpoints, such as binary or time-to-event endpoints, remains open for future research.

Non-concurrent controls share some characteristics with historical controls, as they both refer to data collected prior to the data on the treatment under study, and thus both might introduce bias in the estimates and inflate the type I error rate if included in the analysis [22, 23]. However, compared to historical controls, non-concurrent controls comprise patients who have been part of the same trial framework as the patients allocated to the investigated treatment. Therefore, they typically share the inclusion and exclusion criteria and endpoint assessment procedures [24]. Methods for incorporating historical controls in randomized clinical trials have been widely discussed in the last years, and could be analogously used in the context of platform trials to incorporate NCC data [25]. Frequentist methods include for instance the "test-then-pool" approach, where either separate or pooled analysis is performed based on a frequentist test assessing the equality of the CC and historical data [15]; dynamic pooling, which assigns a weight parameter to the historical data to control their proportion in the analysis [26]; or propensity score methods that can be used to adjust for imbalances in baseline covariates between historical and concurrent controls [27]. Bayesian approaches encompass the power prior method, which down-weights the historical information by introducing a power parameter to their likelihood function [28]; commensurate power prior, an extension to the power prior approach that directly parameterizes the commensurability of the historical and CC data [29]; and meta-analytic-predictive (MAP) prior approaches, which uses the historical information to derive a MAP prior distribution for the CC data [30, 31]. Other Bayesian methods, such as dynamic borrowing, were also proposed for incorporating external data into the trial analysis in order to obtain more information for the decision-making [32, 33]. However, in contrast to the modeling approaches to incorporate NCC data, these methods do not directly adjust for the time trend, but rather down-weight the historical information in order to ameliorate the bias due to heterogeneity in the data. Hence, they still introduce some bias if time trends are present. On the contrary, the model-based approaches for incorporating NCC lead to unbiased estimates provided that the model assumptions are met. A detailed overview of methods discussed in the context of historical, non-concurrent, and/or external controls is provided in the scoping review by Bofill Roig et al. [25].

While analysis using concurrent controls only is still considered the preferred approach, under certain circumstances, such as trials for rare diseases, the use of non-concurrent controls can be valuable [11, 25]. In such cases, methods for addressing the potential bias due to time trends should be employed [11]. The proposed models in this work are in line with these suggestions, increasing the precision of the treatment effect estimators, while mitigating the biases that could arise due to temporal changes.

Supplementary Material Formal definition of the time variables, further specifications of the models, and additional results from the simulation study can be found in the pdf file with supplementary material. The GitHub repository (https://github.com/pavlakrotka/NCC_FreqModels) contains the R code to reproduce the results presented in this paper.

Authors' Contributions M.B.R., M.P. and P.K. conceived this research. G.H. and M.G. established data access and harmonized data across datasets. P.K. prepared the initial draft of the text and performed the simulations and statistical analyses. All authors discussed the results, provided comments and reviewed the manuscript.

Acknowledgments The authors appreciate the insightful comments and suggestions on the application in Section 5 by the IMPROVE-PSP consortium members Mats O. Karlsson and Franz König. This research was funded in whole, or in part, by the Austrian Science Fund (FWF) [ESP 442 ESPRIT-Programm]. For the purpose of open access, the author has applied a CC BY public copyright licence to any Author Accepted Manuscript version arising from this submission. P.K. and M.P. received funding from the European Joint Programme on Rare Diseases (Improve-PSP). G.H. was funded by the Deutsche Forschungsgemeinschaft (DFG, German Research Foundation) under Germany's Excellence Strategy within the framework of the Munich Cluster for Systems Neurology (EXC 2145 SyNergy – ID 390857198) and the European Joint Programme on Rare Diseases (Improve-PSP). M.G. was funded by the European Joint Programme on Rare Diseases (Improve-PSP) and the Swedish Research Council Grant 2018-03317.

This publication is based on research using data from data contributors AbbVie that has been made available through Vivli, Inc. Vivli has not contributed to or approved, and is not in any way responsible for, the contents of this publication.

Conflict of Interest Statement G.H. has ongoing research collaborations with Roche, UCB, Abbvie; serves as a consultant for Abbvie, Alzprotect, Amylyx, Aprinoia, Asceneuron, Bayer, Bial, Biogen, Biohaven, Epidarex, Ferrer, Kyowa Kirin, Lundbeck, Novartis, Retrotope, Roche, Sanofi, Servier, Takeda, Teva, UCB; received honoraria for scientific presentations from Abbvie, Bayer, Bial, Biogen, Bristol Myers Squibb, Esteve, Kyowa Kirin, Pfizer, Roche, Teva, UCB, Zambon; received publication royalties from Academic Press, Kohlhammer, and Thieme.

Other authors have declared no conflict of interest.

Data Availability Statement The data from the ABBV-8E12 trial are available from Vivli - Center for Global Clinical Research Data at https://vivli.org/. Restrictions apply to the availability of these data, which were used under license for the current study, and so are not publicly available. The data from the simulation study and the code to generate the simulated data are available in the GitHub repository https://github.com/pavlakrotka/NCC_FreqModels.

Patient Consent Statement For the ABBV-8E12 trial [19], whose data are used in this reanalysis for the case study, all participants and their respective study partners were required to provide written informed consent before screening or any study specific procedures.

Ethics Approval Statement The ABBV-8E12 trial received independent ethics committee or institutional

review board approval at each study site before initiation. The study adhered to all applicable local regulations, was done in accordance with Good Clinical Practice, as outlined by the International Conference on Harmonisation, and complied with ethical standards described in the Declaration of Helsinki. See [19] for further details. The study protocol for the reanalysis presented in this paper was approved by the ethics committee of the Hannover Medical School, Hanover, Germany (No 9400 BO K 2020) and all methods were performed in accordance with the relevant guidelines and regulations.

Clinical Trial Registration This trial is registered with Clinical Trials.gov, NCT02985879.

References

- [1] Franz Koenig, Cécile Spiertz, Daniel Millar, Sarai Rodríguez-Navarro, Núria Machín, Ann Van Dessel, Joan Genescà, Juan M Pericàs, Martin Posch, Adrian Sánchez-Montalva, et al. Current state-of-the-art and gaps in platform trials: 10 things you should know, insights from EU-PEARL. *Eclinicalmedicine*, 67, 2024.
- [2] Janet Woodcock and Lisa M. LaVange. Master Protocols to Study Multiple Therapies, Multiple Diseases, or Both. New England Journal of Medicine, 377(1):62–70, 2017. ISSN 0028-4793.
- [3] Mary W. Redman and Carmen J. Allegra. The master protocol concept. Seminars in Oncology, 42(5): 724–730, 2015. ISSN 0093-7754. doi: https://doi.org/10.1053/j.seminoncol.2015.07.009.
- [4] Benjamin R. Saville and Scott M. Berry. Efficiencies of platform clinical trials: A vision of the future. Clinical Trials, 13(3):358–366, 2016. ISSN 17407753.
- [5] Elias Laurin Meyer, Peter Mesenbrink, Cornelia Dunger-Baldauf, Hans Jürgen Fülle, Ekkehard Glimm, Yuhan Li, Martin Posch, and Franz Koenig. The Evolution of Master Protocol Clinical Trial Designs: A Systematic Literature Review. Clinical Therapeutics, 42(7):1330–1360, 2020. ISSN 0149-2918. doi: 10.1016/J.CLINTHERA.2020.05.010.
- [6] Kim May Lee, Louise C. Brown, Thomas Jaki, Nigel Stallard, and James Wason. Statistical consideration when adding new arms to ongoing clinical trials: the potentials and the caveats. Trials, 22(1):1–10, 2021. ISSN 17456215. doi: 10.1186/s13063-021-05150-7.
- [7] Lori E. Dodd, Boris Freidlin, and Edward L. Korn. Platform Trials Beware the Noncomparable Control Group. New England Journal of Medicine, 384(16):1572–1573, 2021. ISSN 0028-4793. doi: 10.1056/nejmc2102446.
- [8] Kim May Lee and James Wason. Including non-concurrent control patients in the analysis of platform trials: Is it worth it? *BMC Medical Research Methodology*, 20(1):1–12, 2020. ISSN 14712288. doi: 10.1186/s12874-020-01043-6.
- [9] Marta Bofill Roig, Pavla Krotka, Carl-Fredrik Burman, Ekkehard Glimm, Stefan M Gold, Katharina Hees, Peter Jacko, Franz Koenig, Dominic Magirr, Peter Mesenbrink, et al. On model-based time trend adjustments in platform trials with non-concurrent controls. *BMC medical research methodology*, 22(1): 1–16, 2022.
- [10] Benjamin R Saville, Donald A Berry, Nicholas S Berry, Kert Viele, and Scott M Berry. The bayesian time machine: Accounting for temporal drift in multi-arm platform trials. *Clinical Trials*, 19(5):490–501, 2022. doi: 10.1177/17407745221112013.
- [11] U.S. Food and Drug Administration. Master protocols for drug and biological product development guidance for industry. 2023. https://www.fda.gov/media/174976/download.
- [12] Ian C Marschner and I Manjula Schou. Analysis of adaptive platform trials using a network approach. Clinical Trials, 19(5):479–489, 2022. doi: 10.1177/17407745221112001.

- [13] Paul H.C. Eilers and Brian D. Marx. Flexible smoothing with B-splines and penalties. Statistical Science, 11(2):89–121, 1996. ISSN 0883-4237. doi: 10.1214/SS/1038425655.
- [14] Marta Bofill Roig, Franz König, Elias Meyer, and Martin Posch. Commentary: Two approaches to analyze platform trials incorporating non-concurrent controls with a common assumption. *Clinical Trials*, 19(5):502–503, 2022. doi: 10.1177/17407745221112016.
- [15] Kert Viele, Scott Berry, Beat Neuenschwander, Billy Amzal, Fang Chen, Nathan Enas, Brian Hobbs, Joseph G. Ibrahim, Nelson Kinnersley, Stacy Lindborg, Sandrine Micallef, Satrajit Roychoudhury, and Laura Thompson. Use of historical control data for assessing treatment effects in clinical trials. Pharmaceutical statistics, 13(1):41–54, 2014. ISSN 15391612. doi: 10.1002/pst.1589.
- [16] John P. Matts and John M. Lachin. Properties of permuted-block randomization in clinical trials. Controlled Clinical Trials, 9(4):327–344, 1988. ISSN 0197-2456. doi: 10.1016/0197-2456(88)90047-5.
- [17] Pavla Krotka, Marta Bofill Roig, Katharina Hees, Peter Jacko, and Dominic Magirr. NCC: Simulation and Analysis of Platform Trials with Non-Concurrent Controls, 2023. https://CRAN.R-project.org/package=NCC.
- [18] Pavla Krotka, Katharina Hees, Peter Jacko, Dominic Magirr, Martin Posch, and Marta Bofill Roig. NCC: An R-package for analysis and simulation of platform trials with non-concurrent controls. SoftwareX, 23: 101437, 2023.
- [19] Günter U Höglinger, Irene Litvan, Nuno Mendonca, Deli Wang, Hui Zheng, Beatrice Rendenbach-Mueller, Hoi-Kei Lon, Ziyi Jin, Nahome Fisseha, Kumar Budur, et al. Safety and efficacy of tilavonemab in progressive supranuclear palsy: a phase 2, randomised, placebo-controlled trial. The Lancet Neurology, 20(3):182–192, 2021.
- [20] Lawrence I Golbe and Pamela A Ohman-Strickland. A clinical rating scale for progressive supranuclear palsy. *Brain*, 130(6):1552–1565, 2007.
- [21] Elham Yousefi, Mohamed Gewily, Franz König, Günter Höglinger, Franziska Hopfner, Mats O Karlsson, Robin Ristl, Sonja Zehetmayer, and Martin Posch. Efficiency of multivariate tests in trials in progressive supranuclear palsy. arXiv preprint arXiv:2312.08169, 2023.
- [22] Hans Ulrich Burger, Christoph Gerlinger, Chris Harbron, Armin Koch, Martin Posch, Justine Rochon, and Anja Schiel. The use of external controls: To what extent can it currently be recommended? *Pharmaceutical Statistics*, 20(6):1002–1016, 2021.
- [23] Annette Kopp-Schneider, Silvia Calderazzo, and Manuel Wiesenfarth. Power gains by using external information in clinical trials are typically not possible when requiring strict type i error control. *Biometrical Journal*, 62(2):361–374, 2020.
- [24] Rajeshwari Sridhara, Olga Marchenko, Qi Jiang, Richard Pazdur, Martin Posch, Scott Berry, Marc Theoret, Yuan Li Shen, Thomas Gwise, Lorenzo Hess, et al. Use of nonconcurrent common control in master protocols in oncology trials: report of an American statistical association biopharmaceutical section open forum discussion. *Statistics in Biopharmaceutical Research*, 14(3):353–357, 2022.
- [25] Marta Bofill Roig, Cora Burgwinkel, Ursula Garczarek, Franz Koenig, Martin Posch, Quynh Nguyen, and Katharina Hees. On the use of non-concurrent controls in platform trials: A scoping review. arXiv preprint arXiv:2211.09547, 2022. doi: 10.48550/arxiv.2211.09547.
- [26] Feiran Jiao, Wenda Tu, Sara Jimenez, Victor Crentsil, and Yeh-Fong Chen. Utilizing shared internal control arms and historical information in small-sized platform clinical trials. *Journal of biopharmaceutical* statistics, 29(5):845–859, 2019.
- [27] Heinz Schmidli, Dieter A. Häring, Marius Thomas, Adrian Cassidy, Sebastian Weber, and Frank Bretz. Beyond randomized clinical trials: Use of external controls. *Clinical Pharmacology & Therapeutics*, 107 (4):806–816, 2020. doi: https://doi.org/10.1002/cpt.1723.

- [28] Akalu Banbeta, Joost van Rosmalen, David Dejardin, and Emmanuel Lesaffre. Modified power prior with multiple historical trials for binary endpoints. *Statistics in Medicine*, 38(7):1147–1169, 2019. ISSN 1097-0258. doi: 10.1002/SIM.8019.
- [29] Brian P. Hobbs, Bradley P. Carlin, Sumithra J. Mandrekar, and Daniel J. Sargent. Hierarchical commensurate and power prior models for adaptive incorporation of historical information in clinical trials. *Biometrics*, 67(3):1047–1056, 2011. doi: https://doi.org/10.1111/j.1541-0420.2011.01564.x.
- [30] Heinz Schmidli, Sandro Gsteiger, Satrajit Roychoudhury, Anthony O'Hagan, David Spiegelhalter, and Beat Neuenschwander. Robust meta-analytic-predictive priors in clinical trials with historical control information. *Biometrics*, 70(4):1023–1032, 2014. doi: 10.1111/BIOM.12242.
- [31] Sebastian Weber, Yue Li, John W. Seaman III, Tomoyuki Kakizume, and Heinz Schmidli. Applying Meta-Analytic-Predictive Priors with the R Bayesian Evidence Synthesis Tools. *Journal of Statistical Software*, 100(19):1–32, 2021. doi: 10.18637/jss.v100.i19.
- [32] Dawn Edwards, N Best, J Crawford, L Zi, C Shelton, and A Fowler. Using bayesian dynamic borrowing to maximize the use of existing data: A case-study. *Therapeutic Innovation & Regulatory Science*, 58(1): 1–10, 2024.
- [33] Fulvio Di Stefano, Christelle Rodrigues, Stephanie Galtier, Sandrine Guilleminot, Veronique Robert, Mauro Gasparini, and Gaelle Saint-Hilary. Incorporation of healthy volunteers data on receptor occupancy into a phase ii proof-of-concept trial using a bayesian dynamic borrowing design. *Biometrical Journal*, 65(8):2200305, 2023.

•••

Supplementary material for "Statistical modeling to adjust for time trends in adaptive platform trials utilizing non-concurrent controls"

Pavla Krotka¹, Martin Posch¹, Mohamed Gewily², Günter Höglinger^{3,4,5,6}, and Marta Bofill $Roig^{*1}$

¹Center for Medical Data Science, Medical University of Vienna, Vienna 1090, Austria

²Department of Pharmacy, Uppsala University, Uppsala, Sweden.

³Department of Neurology, LMU University Hospital, Ludwig-Maximilians-Universität (LMU) München, Munich, Germany.

A Formal definition of the time variables

In this section, we present a formal definition of the considered periods, as well as units of calendar time in the platform trial.

We denote by k ($k \in \{1, ..., K\}$) the indicator of the experimental treatment arm, and by s ($s \in \{1, ..., S\}$) and c ($c \in \{1, ..., C\}$) the period and calendar time unit indicator, respectively. For each experimental treatment arm k ($k \in \{1, ..., K\}$), define $\mathbb{P}(k_j = k)$ as the probability that patient j is allocated to this arm. This probability is strictly positive when the arm is active in the trial (i.e. open for randomization when patient j is recruited) and 0 if the treatment arm is not yet or not anymore part of the platform, that is:

$$\mathbb{P}(k_j = k) = \begin{cases} \frac{1}{|\mathcal{K}_A(t_j)| + 1} & \text{if } k \text{ is active} \\ 0 & \text{if } k \text{ is inactive} \end{cases}$$

where $\mathcal{K}_A(t) \subseteq \{1, \dots, K\}$ is the set of active experimental arms at time t. Note that formally, we say that treatment arm k is active at time t if $k \in \mathcal{K}_A(t)$ and inactive otherwise.

We define the entry and exit times of the treatment arm k by t_k^{entry} and t_k^{exit} such that:

$$k \in \mathcal{K}_A(t)$$
 if and only if $t \in [t_k^{entry}, t_k^{exit}]$

Denoting by $\mathbf{t}^{entry,exit} = \{t_1^{entry}, t_1^{exit}, t_2^{entry}, t_2^{exit}, \dots t_K^{entry}, t_K^{exit}\}$ a vector containing the entry and exit times of all experimental arms, we define the end of a period s by t_s^{end} , considering:

$$\begin{split} t_1^{end} &= \min\{t \in \mathbf{t}^{entry,exit} \mid t > 0\} \\ t_s^{end} &= \min\{t \in \mathbf{t}^{entry,exit} \mid t > t_{s-1}^{end}\} \text{ for } s \in \{2,\dots,S\} \end{split}$$

 ⁴ German Center for Neurodegenerative Diseases (DZNE), Munich, Germany.
 ⁵ Munich Cluster for Systems Neurology (SyNergy), Munich, Germany.
 ⁶ Department of Neurology, Hannover Medical School, Hanover, Germany.

^{*}marta.bofillroig@meduniwien.ac.at

where S is the total number of periods in the trial as before.

Finally, the time interval for a period s is given by:

$$T_1^S = [0, t_1^{end}]$$

$$T_s^S = (t_{s-1}^{end}, t_s^{end}] \text{ for } s \in \{2, \dots, S\}$$

The trial can also be divided into equidistant units of calendar time. Given the length of the calendar time interval c_{length} , the trial consists of $C = \min\{x \in \mathbb{N} \mid x \geq t_S^{end}/c_{length}\}$ such intervals. The time interval for a calendar time unit c is then given by:

$$\begin{split} T_1^C &= [0, c_{length}] \text{ for } c = 1 \\ T_c^C &= ((c-1) \cdot c_{length}, c \cdot c_{length}] \text{ for } c \in \{2, \dots, C-1\} \\ T_C^C &= ((C-1) \cdot c_{length}, t_S^{end}] \text{ for } c = C \end{split}$$

B Further specification of the models for treatment-control comparisons

In this section, we provide technical details on the B-spline regression, as well as details on the structure of the covariance matrices in the mixed models with autocorrelated random effects.

B.1 Spline regression

In the spline regression described in Section 2.2, we consider the B-spline function to model the time trend. This function is composed of multiple polynomial functions of a given degree q, which are joined together at points called *knots*, such that the entire spline is continuously differentiable up to the (q-1)th derivative [1].

In our case, the knots are placed within the range of the patient entry times t_j . To define a B-spline function, we first define the knot sequence

$$\zeta_1 = \ldots = \zeta_q = \zeta_{q+1} < \zeta_{q+2} < \ldots < \zeta_{q+Z+1} < \zeta_{q+Z+2} = \zeta_{q+Z+3} = \ldots = \zeta_{2q+Z+2}$$

where the Z knots in the set $\{\zeta_{q+2}, \ldots, \zeta_{q+Z+1}\}$ are called *inner knots*, while ζ_{q+1} and ζ_{q+Z+2} are referred to as *boundary knots*. The additional knots $\{\zeta_1, \ldots, \zeta_q\}$, as well as $\{\zeta_{q+Z+3}, \ldots, \zeta_{Z+2q+2}\}$ are set equal to the boundary knots, even though their choice is essentially arbitrary and only needed because of the later recursive definition of the B-spline [2].

The function $f(t_i)$ can then be represented by a set of basis functions $B_i^q(t_i)$ as follows [3]:

$$f(t_j) = \sum_{i=1}^{q+Z+1} B_i^q(t_j)\beta_i$$

where β_i are the associated regression coefficients and the functions $B_i^q(t_j)$ are defined using the following formula, recursive in q, as follows:

$$B_i^q(t_j) = \frac{t_j - \zeta_i}{\zeta_{i+q} - \zeta_i} B_i^{q-1}(t_j) + \frac{\zeta_{i+q+1} - t_j}{\zeta_{i+q+1} - \zeta_{i+1}} B_{i+1}^{q-1}(t_j), \qquad i = 1, \dots, q + Z + 1$$

with

$$B_i^0 = \begin{cases} 1 & \zeta_i \le t_j < \zeta_{i+1} \\ 0 & \text{otherwise} \end{cases}$$

and

$$B_i^0 \equiv 0$$
 if $\zeta_i = \zeta_{i+1}$

As described in the main paper, we evaluate two strategies for the positions of the inner knots $\{\zeta_{q+2},\ldots,\zeta_{q+Z+1}\}$. Firstly, we place the inner knots to the beginning of each period $s=2,\ldots,S$, such that one polynomial of degree q is always fitted to each period. In this case, the number of inner knots Z=S-1. Moreover, we consider placing the inner knots equidistantly, according to the length of the calendar time unit, and thus fitting a polynomial of degree q to each calendar time interval, which leads to Z=C-1. The boundary knots ζ_{q+1} and ζ_{q+K+2} are always set to 1 and N, respectively, hence to the beginning and end of the trial.

B.2 Mixed-effect models with autocorrelated random effects

In the mixed-effect models with autocorrelated random effects, described in Section 2.3, the random effects u_s for individual periods are assumed to follow a normal distribution with mean 0, constant variance σ_{period}^2 and an AR(1) correlation structure, i.e.:

$$\boldsymbol{u} \sim \mathcal{N}(0, \sigma_{period}^2 \cdot \Sigma_{S_M \times S_M})$$

$$\Sigma_{S_M \times S_M} = \begin{bmatrix} 1 & \phi & \cdots & \phi^{S_M - 1} \\ \phi & 1 & \cdots & \phi^{S_M - 2} \\ \vdots & \vdots & \ddots & \vdots \\ \phi^{S_M - 1} & \phi^{S_M - 2} & \cdots & 1 \end{bmatrix}$$

An analogous distribution is assumed for the random effects u_c associated with different calendar times:

$$oldsymbol{u} \sim \mathcal{N}(0, \sigma_{calendar}^2 \cdot \Sigma_{C_M imes C_M})$$

$$\Sigma_{C_M \times C_M} = \begin{bmatrix} 1 & \phi & \cdots & \phi^{C_M - 1} \\ \phi & 1 & \cdots & \phi^{C_M - 2} \\ \vdots & \vdots & \ddots & \vdots \\ \phi^{C_M - 1} & \phi^{C_M - 2} & \cdots & 1 \end{bmatrix}$$

The parameter ϕ denotes the correlation between two adjacent periods or calendar time units. Note that ϕ can range from -1 to 1 and the correlation of periods that are w units apart is equal to ϕ^w , such that the correlation is weaker for periods or calendar time units that are further apart.

C Additional Results

Figure S1: Setting 1A: Type I error rate and power of the fixed effect regression model with period adjustment compared to the pooled and separate analyses with respect to the strength of the time trend λ . In this example, d = 400 and n = 250 in each experimental arm and a linear shape of the time trend are used. Results for different experimental arms are shown in the rows.

Figure S2: Setting 1A: Type I error rate and power of the fixed effect regression model with period adjustment compared to the pooled and separate analyses with respect to the timing of adding the treatment arms. In this example, n = 250 in each experimental arm and a linear time trend with strength $\lambda = 0.5$ are considered. Results for different experimental arms are shown in the rows.

Figure S3: Setting 1A: Type I error rate and power of the regression model with period adjustment compared to the pooled and separate analyses with respect to the index of the evaluated arm. Here, d = 200, n = 250 in each experimental arm, and a linear time trend with strength $\lambda = 0.5$ are considered.

Figure S4: Setting 1B: Type I error rate and power for the spline regression model with knots according to periods or calendar time units compared to the regression model with period adjustment with respect to the strength of the time trend λ using different time trend patterns. In this example, n=250 in each experimental arm and $N_p=1660$ in case of inverted-U trend (corresponding to the middle of the trial) are used. In case of calendar time adjustment, unit size of 100 patients is considered. Treatment arm 5 is being evaluated. Results for different degrees of the polynomial spline (linear, quadratic, cubic) are shown in the rows.

Figure S5: Setting 1B: Type I error rate and power for the cubic spline regression model with knots according to periods or calendar time units compared to the regression model with period adjustment with respect to the strength of the time trend λ using different time trend patterns. In this example, n=250 in each experimental arm, $N_p=1660$ in case of inverted-U trend (corresponding to the middle of the trial) are used. In case of calendar time adjustment, unit size of 100 patients is considered. Results for different experimental arms are shown in the rows.

Figure S6: Setting 2A: Type I error rate and power of the regression model with calendar time adjustment compared to the regression model with period adjustment and separate analysis with respect to the size of the calendar time unit under different time trend patterns. In this example, n = 250 in each experimental arm, $\lambda = 0.125$ and $N_p = 750$ in case of inverted-U trend (corresponding approximately to the middle of the trial) are considered. Results for different experimental arms are shown in the rows.

Figure S7: Setting 2A: Type I error rate and power of the regression model with calendar time adjustment compared to the regression model with period adjustment and separate analysis with respect to the strength of the time trend λ under different time trend patterns. In this example, n=250 in each experimental arm, $N_p=750$ in case of inverted-U trend (corresponding approximately to the middle of the trial) and calendar time unit size of 100 are used. Results for different experimental arms are shown in the rows.

Figure S8: Setting 2B: Type I error rate and power of the mixed model with period and calendar time

adjustments as uncorrelated and autocorrelated random effects, compared to the fixed effect regression model with period adjustment with respect to the pattern and strength of the time trend. Sample sizes of n=250 in each experimental arm, $N_p=750$ in case of inverted-U trend (corresponding approximately to the middle of the trial) are used. In case of calendar time adjustment, unit size of 100 patients is considered. Results for different experimental arms are shown in the rows.

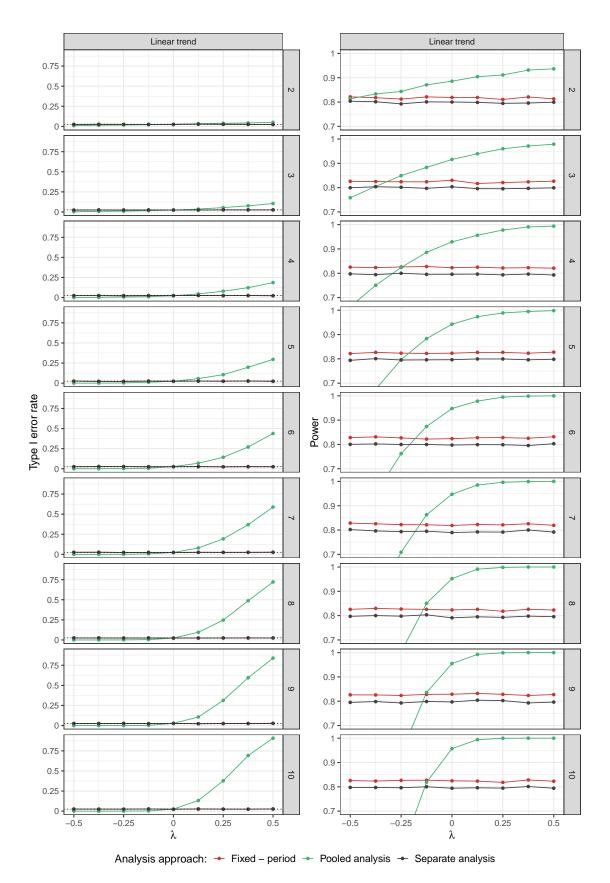


Figure S1

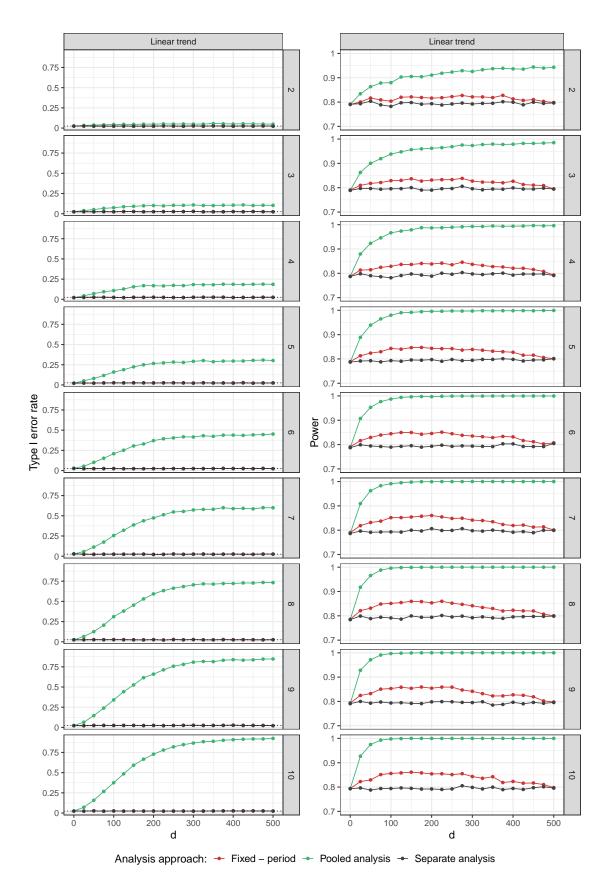


Figure S2

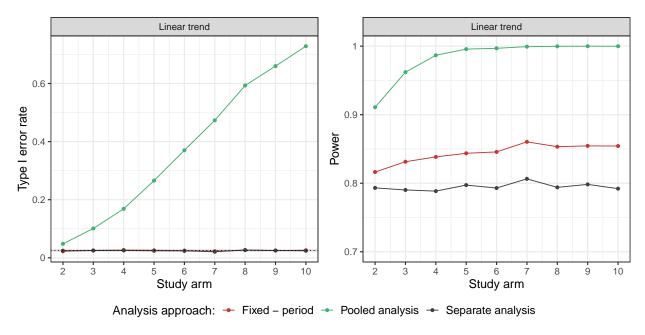
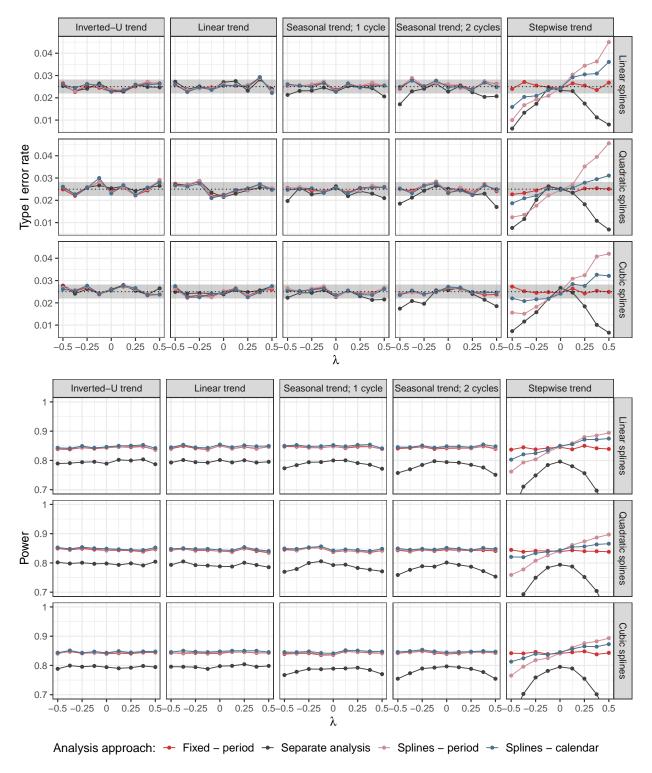


Figure S3



 $Figure \ S4$

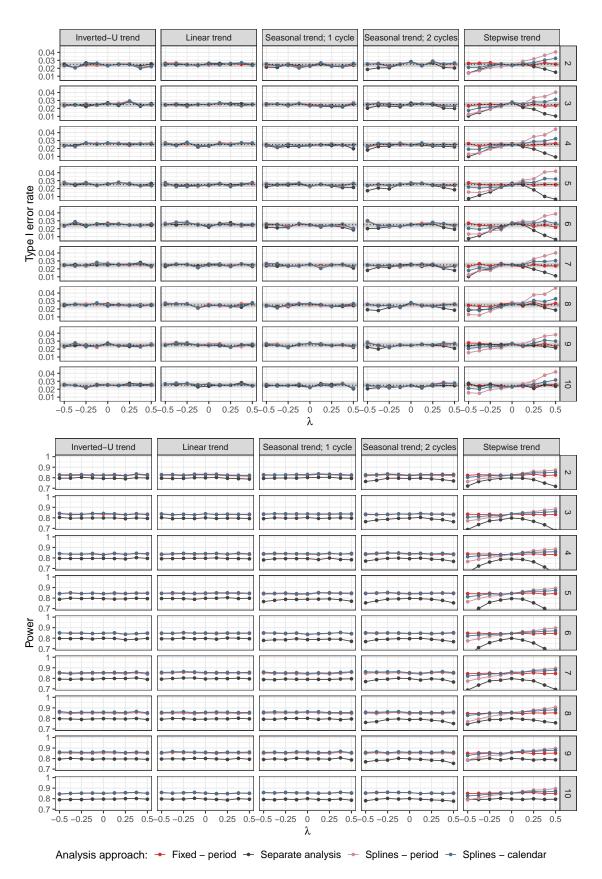
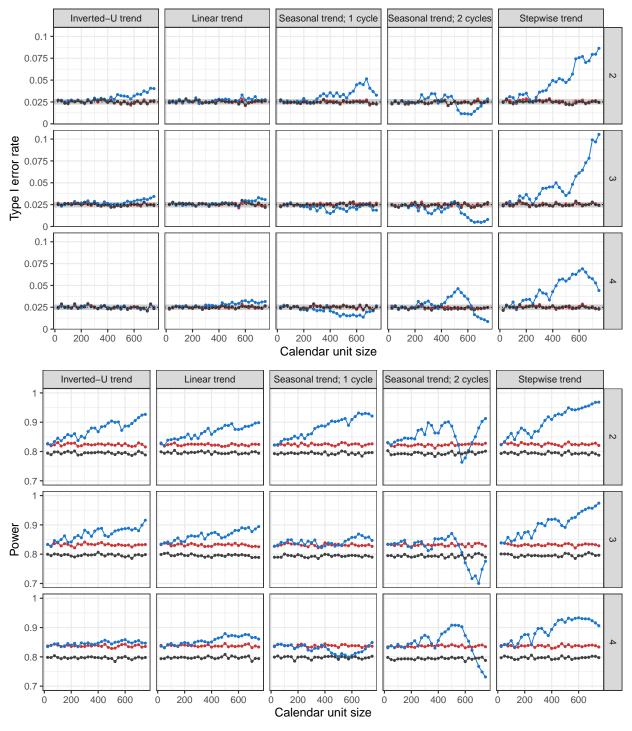
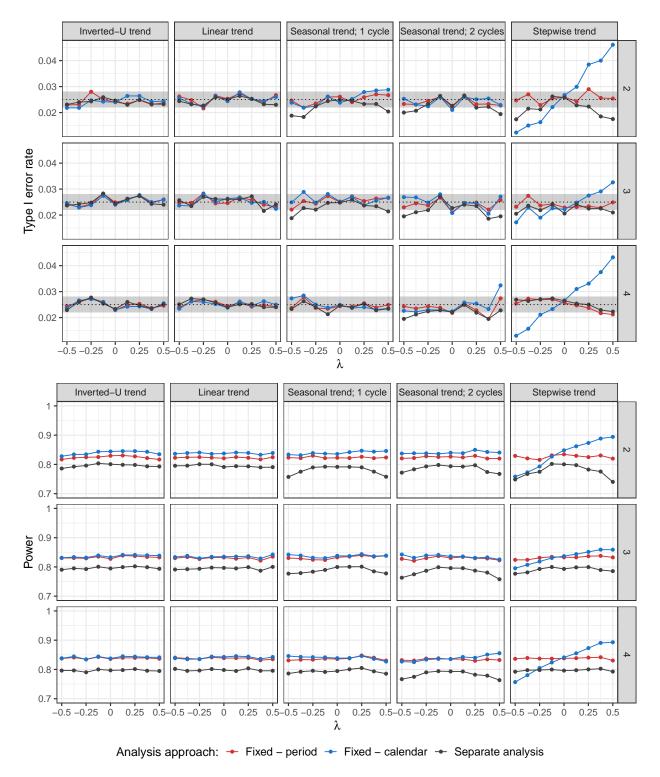


Figure S5



Analysis approach: → Fixed – period → Fixed – calendar → Separate analysis

 $Figure \ S6$



 $Figure\ S7$

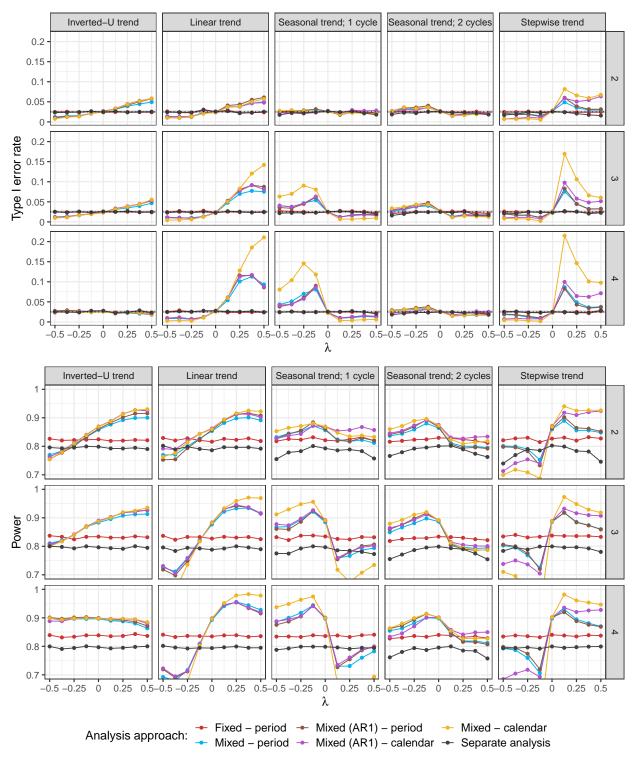


Figure S8

References

- [1] Paul H.C. Eilers and Brian D. Marx. Flexible smoothing with B-splines and penalties. *Statistical Science*, 11(2):89–121, 1996.
- [2] Aris Perperoglou, Willi Sauerbrei, Michal Abrahamowicz, and Matthias Schmid. A review of spline function procedures in R. *BMC Medical Research Methodology*, 19(1):1–16, 2019.
- [3] Simon N. Wood. Generalized Additive Models: An Introduction with R. Chapman and Hall/CRC, 2017.